

# Aggregation and Dispersion of Colloidal Suspensions by Inorganic Surfactants: Effect of Chemical Speciation and Molecular Conformation

Jun Liu,\* Li-Qiong Wang, William D. Samuels, and Gregory J. Exarhos

Pacific Northwest National Laboratory, Richland, Washington 99352

Received: May 15, 1997; In Final Form: July 24, 1997<sup>⊗</sup>

Polyphosphates are widely used as inorganic dispersants, but the mechanism of the dispersing is not well understood. In this study, the colloidal properties of fine alumina suspensions in water were studied at different pH conditions in the presence of linear chain polymetaphosphates. The chemical speciation and molecular conformation were probed using liquid and solid state  $^{31}\text{P}$  and  $^{27}\text{Al}$  nuclear magnetic resonance spectroscopy. Three regimes have been found: (i) Neutral pH—long-chain metaphosphates are partially anchored to the alumina surface. The negatively charged metaphosphate molecules extend from the particle surface to the solution to provide an effective electrosteric repulsion force that acts to disperse the colloidal particles. (ii) Low pH—the alumina particle surfaces hydrolyze and the dissolved species react with the surfactant to form amorphous aluminum phosphate gels. The reaction product causes bridging flocculation of the suspension. (iii) High pH—partial dissolution of alumina produces tetrahedrally bonded hydroxylaluminate anions, which induces the long-chain polymetaphosphates to dissociate into phosphate anions. Under these conditions, the metaphosphate no longer exhibits dispersion properties. A fundamental understanding of the particle–surfactant interactions in terms of adsorption, chemical reaction, and molecular conformation will provide insights for the rational design of more effective inorganic dispersants.

## Introduction

Inorganic surfactants, such as polymetaphosphates, have been known to be effective dispersants for ceramic suspensions.<sup>1,2</sup> However, the effectiveness of the dispersing action depends on the solution conditions (pH values) and aging time. Although a vast amount of knowledge has accumulated for organic dispersants, the properties of inorganic surfactants in ceramic suspensions is not well understood. Dispersion with an organic surfactant depends on the adsorption of molecules, the charging behavior, and the molecular conformation.<sup>3–6</sup> The dispersant either provides (i) an electrostatic interaction if the adsorbed molecules are charged, (ii) a repulsive steric force when the adsorbed molecules extend from the particle surface to the solution, or (iii) an electrosteric interaction that combines the electrostatic and steric effects.<sup>7</sup> These repulsive forces keep the particles separated in the suspension. Such a systematic understanding is not available for inorganic dispersants. One key question concerns the relative importance of the steric interaction since inorganic surfactants often are smaller than commercially used organic dispersants. Furthermore, the inorganic dispersants not only ionize in the solution, but they are also susceptible to hydrolysis and can chemically react with other ceramic phases. The consequences of such chemical processes have not been carefully studied.

Two mechanisms have been proposed for particle dispersions involving polyphosphates:<sup>1</sup> sequestering of multivalent ions and complexation with the colloidal particle surface. For negatively charged particle surfaces, the metaphosphates are assumed to only bind multivalent cations such as  $\text{Ca}^{2+}$  and  $\text{Mg}^{2+}$ , which otherwise would preferentially adsorb to the double layer and reduce the surface potential to cause flocculation. For positively charged particles, the metaphosphate anions adsorb on the surface and provide an effective double layer that promotes colloidal stability. It has also been reported<sup>1</sup> that aging in aqueous solutions induces the polyphosphate anions to dissociate

into shorter chains, thus reducing the effectiveness of the surfactant.<sup>3</sup> However, these mechanisms do not adequately address the complicated behavior of the inorganic dispersants in ceramic suspensions.

A good understanding of particle–surfactant interactions in terms of adsorption, chemical reaction, and molecular conformation will provide insights for the rational design of more effective inorganic dispersants. Inorganic dispersants have attracted great attention as ceramic processing aids because the surfactants themselves can be incorporated into the ceramic matrix.<sup>8,9</sup> When organic surfactants are used in the colloidal ceramic processing (mixing, dispersing, and forming) stages, they have to be removed later by thermal decomposition. This process causes materials to shrink and generates gaseous wastes.<sup>3</sup> The inorganic dispersants as an alternative processing aid will eliminate or reduce these problems because the majority of the inorganic surfactants will be converted to ceramic materials. Well-defined alumina particles and polymetaphosphates were chosen as the model system for this study. Alumina is the mostly widely encountered ceramic material. Metaphosphates were selected because they have a linear chain conformation that is similar to many organic dispersants used in ceramic processing, such as the alkyl carboxylic acids among polyelectrolytes.<sup>9</sup>

## Experimental Section

The alumina particles used in this study were high-purity (999.995%) Sumitomo AKP 53. The mean particle diameter was  $0.2\ \mu\text{m}$ , and the specific surface area was  $9\text{--}15\ \text{m}^2/\text{g}$ . Linear chain polymetaphosphates, with the general formula  $(\text{NaPO}_3)_n$ , were from FMC Corporation (Philadelphia, PA). Two chain lengths were investigated. For Sodaphos, the average chain had 6 phosphorus atoms ( $n = 6$ ), and for Glass H, the average chain contained 21 phosphorus atoms ( $n = 21$ ). The data on the chain lengths was supplied by the manufacturer and confirmed

<sup>⊗</sup> Abstract published in *Advance ACS Abstracts*, September 15, 1997.

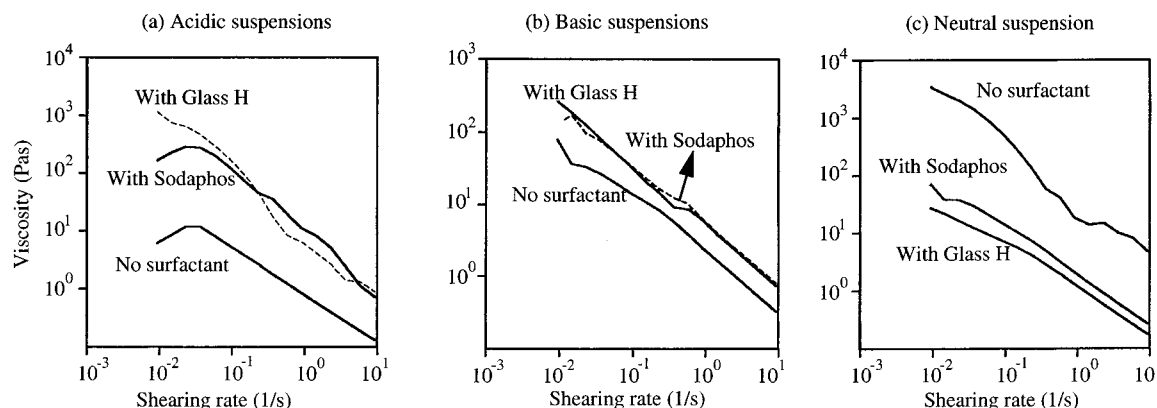


**Figure 1.** Viscosities of alumina suspensions with and without surfactants at different pH values. (a) Acidic suspensions. Adding polymetaphosphate surfactants greatly increased the viscosities of the suspensions. (b) Basic suspensions. Adding the surfactants moderately increased the viscosities. (c) Neutral suspensions. Adding the surfactants greatly reduced the viscosity. Glass H is more effective than Sodaphos in reducing the viscosities.

by our nuclear magnetic resonance (NMR) experiments (to be discussed later). To determine the  $\zeta$  potential, the viscosity of alumina suspensions was measured as a function of phosphate concentration at several pH conditions. Solid state  $^{27}\text{Al}$  and  $^{31}\text{P}$  NMR spectra were obtained for identical samples.

Suspensions (380 mL) containing 2 vol % alumina were prepared by mixing 30 g of AKP alumina and 372 mL of deionized water. The pH of each suspension was adjusted by 1 M  $\text{HNO}_3$  or 1 M  $\text{NaOH}$ . The suspension was loaded into the sample container of an AcoustoSizer (Matech Applied Science) under continuous mechanical stirring. Small amounts of metaphosphates were added to the suspension, and the  $\zeta$  potential of the alumina particles was measured as a function of the phosphate concentration. A roughly 10 min lag time was used between each addition of the phosphate to allow the suspension to equilibrate.

For viscosity measurement, alumina suspensions (20 vol %) were prepared in 0.1 M  $\text{NaNO}_3$  solutions. The pH values of the suspensions were adjusted using 1 M  $\text{HNO}_3$  and 1 M  $\text{NaOH}$ . Appropriate amounts of phosphates were weighed into the suspensions to give a phosphate concentration of 3 wt % of the alumina content. The viscosities of the suspensions were measured using a Bohlin VOR Rheometer (by Bohlin Instruments) under unidirectional shearing from 0.01 to 10 1/s with a cone/cup geometry.

The 120.78 MHz  $^{31}\text{P}$  NMR experiments were carried out with a Chemagnetics spectrometer (300 MHz, 89 mm wide bore Oxford magnet) using a variable-temperature double-resonance probe. For surfactant/alumina gels, single-pulse (SP) Bloch-decay and cross-polarization (CP) methods with magic angle spinning (MAS) were used with  $^1\text{H}$  decoupling. The surfactant/alumina gels were loaded into 7 mm zirconia rotors and spun at 4 kHz. The same rotors were used for the pure surfactant solutions without spinning. The suspensions (pastelike samples) were capped by two end caps to prevent the samples from drying during experiments. Spectra were collected by using an SP excitation Bloch-decay method with a 5  $\mu\text{s}$  ( $90^\circ$ )  $^{31}\text{P}$  pulse and a 30 s repetition delay. A 164 ms acquisition time and a 25 kHz spectral window were employed for all experiments. The power levels of the phosphorus and proton channels were set so that the Hartmann–Hahn match was achieved at 55 kHz in CP experiments. A Lorentzian line broadening of 24 Hz was used for all MAS NMR spectra. The  $^{31}\text{P}$  chemical shifts were referenced to the 0 ppm signal using 85%  $\text{H}_3\text{PO}_4$  as the external standard. SP Bloch-decay 77.74 MHz  $^{27}\text{Al}$  NMR spectra were taken for pastelike samples and solutions under nonspinning conditions. The  $^{27}\text{Al}$  chemical shifts were referenced to the 0 ppm signal using 0.1 M  $\text{Al}(\text{NO}_3)_3$  as the external standard.

## Results

**Viscosity of the Alumina Suspensions.** The background electrolyte concentrations of all the suspensions for viscosity measurement were adjusted to 0.1 M by  $\text{NaNO}_3$ . The acidic suspensions were prepared as follows: a 20 vol % alumina suspension was prepared first, and the pH value of the suspension was adjusted to 1.87. This suspension was then separated into three parts. 3 wt % Sodaphos (per gram of alumina) was added to one part, and 3 wt % Glass H was added to another part. Similar methods were used to prepare the basic suspensions, except that the pH of the initial suspension was first adjusted to 11.62 with 1 M  $\text{NaOH}$ . The neutral suspensions were prepared by mixing alumina and deionized water. The as-prepared suspension has a pH value between 6 and 7. The pH value of the neutral suspensions increased to between 9 and 10 when the phosphate surfactant was added to the suspension. For the acidic and basic suspensions, the pH values of the suspensions did not change significantly when the metaphosphates were added ( $<0.5$  pH unit).

Figure 1a–c shows the viscosities of the 20-vol % alumina suspensions as a function of shearing rate at different pH conditions with and without the metaphosphate surfactants. At low pH, adding both the Sodaphos and the Glass H caused the viscosity of the suspensions to increase by 1–2 orders of magnitude, and the viscosities with Sodaphos and Glass H are similar. At high pH, adding the metaphosphate surfactants caused the viscosity to increase moderately. Again, the chain length of the surfactant has little effect. Sodaphos and Glass H gave the same results. The metaphosphates functioned as dispersing agents only in neutral pH ranges, and the viscosities of the suspensions were reduced by more than 1 order of magnitude. The long-chain molecule, Glass H ( $n = 21$ ), was found to produce a lower viscosity than the short-chain molecule, Sodaphos ( $n = 6$ ).

**NMR Results.** NMR spectroscopy was used to probe the observed rheological behavior of the suspensions containing metaphosphate surfactants.

(i)  $^{31}\text{P}$  NMR of Pure Phosphate Solutions. First,  $^{31}\text{P}$  liquid-state NMR spectra for 10 wt % Sodaphos and Glass H solutions (prepared by adding metaphosphate to deionized water) at different pH conditions were obtained, and the results are given in Figure 2 where features located in two well-separated spectral regions are seen. On the basis of previous work,<sup>10–13</sup> the resonances at  $-20$  to  $-23$  ppm are assigned to the phosphorus atoms associated with the middle-chain groups. Resonances at  $-10$  to  $-4.7$  ppm are attributed to phosphorus atoms associated with the end-chain groups. Because the resonances

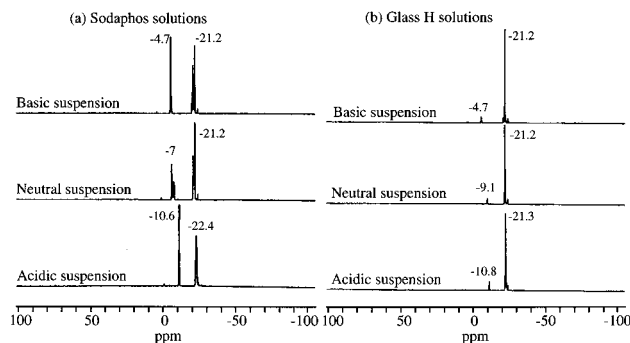


**Figure 2.** SP  $^{31}\text{P}$  NMR spectra of pure surfactant solutions (without alumina particles): (a) Sodaphos solutions; (b) Glass H solutions. The peak from  $-4.5$  to  $-11$  ppm corresponds to the end-chain group, and the peak at approximately  $-22$  ppm corresponds to the middle-chain group. The pure surfactant solutions were stable at room temperature. No change was observed in the NMR spectra after 7 days.

associated with end-chain and middle-chain groups are distinct, we can estimate the oligomer chain length from the relative peak areas of the two groups. The peak area ratios between the signals from the end-chain and the middle-chain groups should be 2:4 and 2:19 for Sodaphos (6 phosphorus atoms in a chain) and for glass H (21 phosphorus atoms in a chain), respectively. The ratios obtained by integrating the peak areas in Figure 2 agree well with the chain length data supplied by the manufacturer. A small amount of orthophosphate was also found for Sodaphos solutions shown in Figure 2 in the region from 0 to 6 ppm as impurities in the as-supplied materials. Changing the pH conditions of the metaphosphate solutions was found to have little effect, and no shifts were observed for the middle-chain groups. However, the resonances associated with the end-chain groups shift downfield several parts per million as the pH increases. This shift can largely be attributed to the changes in the end groups from  $-\text{P}-\text{OH}$  at low pH to  $-\text{P}-\text{ONa}$  at high pH.

Previous work suggested that aging polyphosphates in aqueous solutions caused hydrolysis and decomposition and reduced the effectiveness of the dispersing agent.<sup>1</sup> In our experiments, the pure phosphate solutions were stable at least up to 7 days, and no change was observed in  $^{31}\text{P}$  NMR spectra (not shown in the paper) for these two surfactant solutions after aging at room temperature for 1–7 days. Another study<sup>14</sup> reported the obvious spectral changes in sodium trimetaphosphate (STP) solutions indicating the formation of orthophosphate and pyrophosphate, but these changes were only observed at a higher temperature of  $53^\circ\text{C}$  after a long period (40 days). Therefore, it is safe to assume that in the solutions that do not contain alumina colloids, the polymetaphosphate chains do not degrade at room temperature or as a function of pH.

(ii)  $^{31}\text{P}$  NMR of Alumina–Phosphate Suspensions. To prepare NMR samples, the alumina suspensions were centrifuged at 15 000 rpm. Solid-state MAS NMR measurements were performed on the sediments and/or supernatants. To prevent drying-induced chemical changes in the NMR experiments, the sample cells were carefully sealed. Figure 3 gives SP spectra with proton decoupling for the suspensions with Sodaphos and Glass H under different pH conditions, and Figure 4 gives the CP spectra for the same samples. Figure 3 exhibits both the sharp resonances associated with solvated species and the broad resonance associated with the species that are less mobile. Because CP is a measure of the efficiency of magnetization transfer by the dipolar coupling from  $^1\text{H}$  to  $^{31}\text{P}$ , the relative peak intensities for individual phosphorus groups in the CP spectra reflect both the magnitude of the dipolar coupling and motions of the  $\text{P}-\text{H}$  vector.<sup>15,16</sup> Resonances

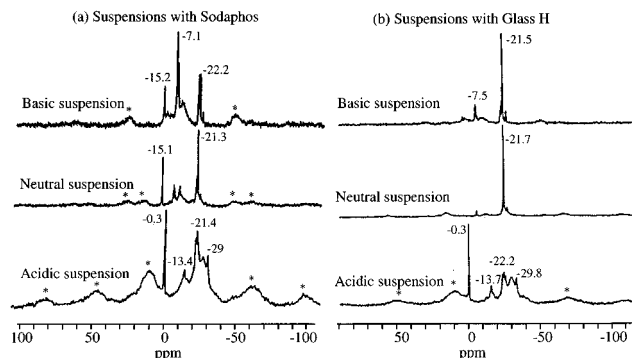


**Figure 3.** SP  $^{31}\text{P}$  NMR spectra of alumina suspensions with surfactants: (a) with Sodaphos at different pH values; (b) with Glass H at different pH values. The peaks labeled by \* are spin-sidebands. At low pH, many broad spectral features are observed from  $-13$  to  $-36$  ppm, corresponding to different binding environments of the phosphorus with respect to aluminum. These broad spectral features are not present at neutral and high pH values.

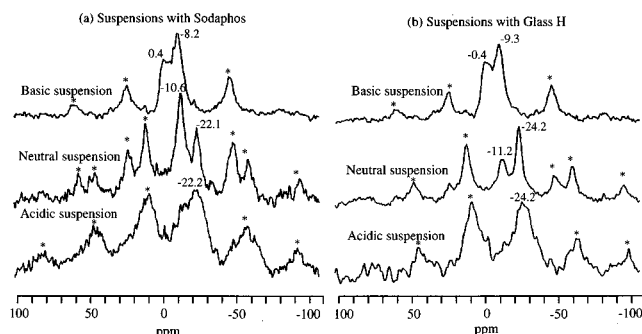


**Figure 4.** CP  $^{31}\text{P}$  NMR spectra of alumina suspensions with surfactants: (a) with Sodaphos at different pH values; (b) with Glass H at different pH values. At low pH, only a broad peak is observed, suggesting the formation of immobile species with chemical heterogeneity. At neutral pH, the peaks from the end group and the middle groups are well resolved. At high pH, the spectra show the peaks corresponding to the end group and orthophosphate, suggesting dissociation of large molecules into smaller ones.

associated with solvated species were not observable in CP spectra because such species are mobile. The sharp resonances associated with solvated surfactant in SP spectra shown in Figure 3 disappeared in the CP spectra shown in Figure 4. Clearly, the advantage of using CP methods here is to probe only the adsorbed surfactants in the alumina/phosphate suspensions. Besides, it is difficult to determine the peak positions for adsorbed surfactants from SP spectra because signals from the solvated surfactants overlapped with those from the adsorbed surfactants.

From the approximate estimate of the peak area (Figure 3), the fraction of solvated species in all surfactant/alumina samples was found to be much less than that for the adsorbed surfactants. Figure 3 also shows that the intensities of the resonances associated with solvated surfactants in a surfactant/alumina sample at pH 2 are much less than the analogous signals for samples at pH 7 and 11. Instead, several broad resonance peaks can be observed from  $-13$  to  $-40$  ppm due to the existence of immobile species. This result is consistent with a previous study<sup>17</sup> on the mixing of sodium polyphosphate and aluminum nitrate at low P/Al ratios. Similar peak positions and peak shapes were reported. The spectral features from  $-13$  to  $-15$  ppm were assigned to the Al-bound bidentate, unprotonated end group. Features at  $-23$  to  $-28$  ppm were assigned to the Al-bound middle-chain group, and the features at  $-30$  to  $-36$  ppm to the Al-bound monodentate middle-chain phosphate groups. These assignments were based on the argument that the

deshielding of P atoms upon binding to alumina surfaces results in an upfield shift of the peak position for bound phosphate relative to that for unbound phosphate. In our experiments, the resonances associated with both the end-chain and middle-chain groups for immobile surfactants at pH 2 exhibit an upfield shift at 2–5 ppm, indicating likely surface binding.

The influence of pH on alumina–metaphosphate suspensions is illustrated in CP MAS spectra shown in Figure 4. Spectra for both Sodaphos and Glass H at pH 2 only exhibited a broad resonance (–20 ppm). The features in CP spectra for the pH 2 suspensions in Figure 4 are less well resolved as compared with the SP spectra under the same conditions. A single broad resonance peak seen in CP spectra also suggests the formation of immobile species with chemical inhomogeneity. CP spectra taken at a neutral pH range show two well-resolved peaks at –11 and –22 ppm, corresponding to the end and middle groups, respectively. The position of the resonance associated with the end-chain group shifted upfield 2–3 ppm, and the position of the middle group remained the same as compared with colloid free surfactant solutions. This suggests that the middle-chain groups were not affected by binding, but the end-chain groups were bound to the particle surface, most likely through hydrogen bonding. At pH 12, CP spectra show two resonance peaks at 0 and –9 ppm, corresponding to orthophosphate and the end-chain groups, respectively (Figure 4). The observation of a substantial amount of bound orthophosphate and the enhanced peak intensity from the end-chain groups indicate that some of metaphosphates had undergone hydrolysis and dissociation in high-pH alumina suspensions. This process reduced the chain length of the surfactants. The significant reduction in the intensity of the middle group may be attributed to several factors. First, fraction of the polymetaphosphate molecules dissociated into shorter chain polyphosphates (eg.,  $P_2O_7^{4-}$ , etc.), resulting in a reduced signal from the middle-chain group. Second, CP methods depend on the efficiency of the proton transfer. At high pH, most phosphates are deprotonated. When fewer protons are near the phosphorus, the peak intensity in CP spectra would be significantly decreased. The upfield shifts for the resonances associated with the end-chain groups suggest that the end-chain groups are bound to the alumina surface, probably through sodium ions.

(iii) *<sup>27</sup>Al NMR Experiments.* Further information is provided by <sup>27</sup>Al NMR on the behavior of the alumina/phosphate suspensions. At low pH, alumina is susceptible to hydrolysis and dissolution. The dominant soluble species are hydrated  $Al(H_2O)_6^{3+}$  ions and  $Al_{13}O_4(H_2O)_{12}^{7+}$  clusters ( $Al_{13}$  clusters). The  $Al_{13}$  cluster contains 12  $AlO_6$  octahedra joined by common edges, with a tetrahedral aluminum atom at the center.<sup>18–20</sup> The existence of these species in pure alumina suspensions is revealed in the NMR spectrum shown in Figure 5a. The broad hump from –75 to 75 ppm is from the signal of the undissolved alumina particles under the nonspinning condition. The small peak at 10 ppm comes from some unidentified surface species. The peak at 0 ppm corresponds to single aluminum ions, and the peak at 65 ppm corresponds to the  $Al_{13}$  clusters. After the metaphosphate surfactant is added to the alumina suspensions, the two narrow resonances at 0 and 65 ppm disappear (Figure 5b), and new resonance peaks appear at –3 and –6 ppm. The peaks at –3 and –6 ppm can be assigned to aluminum phosphate.<sup>17</sup> Therefore, the interaction at low pH can be summarized as follows: the alumina particles partially dissolved into the solution to form soluble Al ions and  $Al_{13}$  clusters. These soluble species interact with phosphate surfactants to form various kinds of aluminum phosphates, which precipitated out of the solution. This drove the reaction to further dissolution

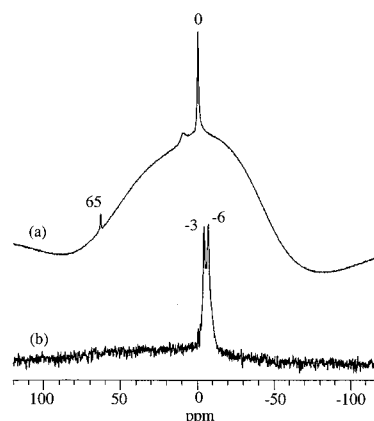


**Figure 5.** <sup>27</sup>Al NMR spectra of alumina suspensions at low pH. (a) Without surfactants. The peaks at 0 and 65 ppm correspond to  $Al^{3+}$  ions and  $Al_{13}$  clusters of the dissolved aluminum species. (b) With surfactants. The peaks from dissolved aluminum disappear, and new peaks at –3 and –6 ppm suggest the formation of aluminum phosphate phases. This spectrum is obtained from the supernatant.

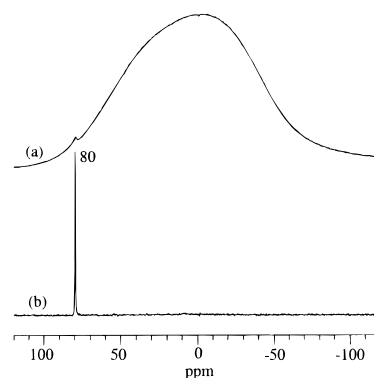


**Figure 6.** <sup>27</sup>Al NMR spectra of alumina suspensions at high pH. The peak at 80 ppm indicates that sodium aluminate is formed. (a) NMR spectrum obtained from the sediment. (b) NMR spectrum obtained from the supernatant.

and formed more insoluble aluminum phosphates. The precipitated aluminum phosphates most likely are amorphous and therefore would have a distribution of chemical bonding environment (bond angles, bond lengths).<sup>17</sup>

In the neutral pH range, alumina is not soluble, and the NMR spectrum only showed one broad peak from –75 to 75 ppm (data not shown), corresponding to the solid phase. Under this condition, the particles were not highly charged; the only mechanism by which such particles can interact with the metaphosphate surfactant is through hydrogen bonding.

At high pH, the <sup>13</sup>Al spectrum for the polymetaphosphate/alumina suspension in Figure 6 exhibits a sharp resonance line at 80 ppm, which is assigned to the tetrahedrally bonded hydroxylaluminate species,  $[Al(OH)_4]^-$ . This finding agrees with previous work and NMR line assignments,<sup>20,21</sup> which indicate that strong base attacks alumina (octahedrally coordinated  $Al^{3+}$ ) rendering it soluble in water through formation of the tetrahydroxy complex.

On the basis of the the formation of this species, one proposed mechanism for surfactant chain dissociation involves condensation of the hydroxylaluminate species with the –OH groups resident on the polymetaphosphate chain ends. In the absence of alumina, NMR evidence showed long-term stability (1 week) of the surfactant chains even in highly basic media. CP NMR evidence indicates that a fraction of the surfactant terminal groups are still protonated since a well-resolved phosphorus peak associated with the terminal groups is observed in Figure 4 (CP is a measure of the magnetization transfer resulting from dipolar

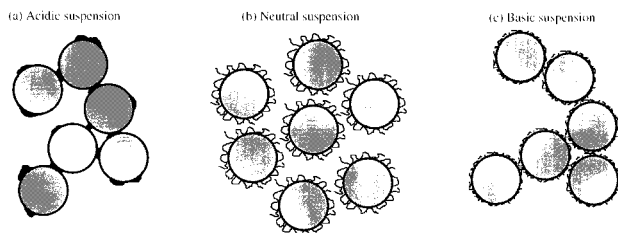


**Figure 7.** Schematic illustration of dispersing and flocculation mechanism of the polymetaphosphate surfactants. (a) Bridging flocculation at low pH due to the formation of aluminum phosphate gel phases. (b) Electrosteric stabilization from negatively charged long-chain surfactants extending from the particle surfaces into the solution. (c) Decomposition of long-chain surfactants into shorter ones and flocculation due to compressed electrical double layers.

coupling between  $^1\text{H}$  and  $^{31}\text{P}$ ). Following condensation, the terminal phosphate group on the surfactant is split off and the newly formed terminal phosphate group on the surfactant chain becomes hydroxylated. The CP signal remains well resolved for days, indicating that the dynamic equilibrium established still favors localization of terminal hydroxyl groups on the surfactant chains. This mechanism, based upon the measured NMR data, requires the formation of hydroxyaluminate groups that selectively remove terminal phosphate groups from the surfactant chains, thereby reducing their length as a function of time. Work is in progress to further address the mechanism for the chain scission reaction in high-pH solutions.

## Discussion

The NMR results can be used to explain the colloidal stability of aqueous alumina suspensions with and without the addition of metaphosphate surfactants. Simple models illustrating flocculation and dispersion phenomena in aqueous suspensions containing metaphosphate surfactants are shown in Figure 7.

At low pH, the hydrolysis of alumina produced hydrated Al ions and  $\text{Al}_3$  clusters. These soluble species interacted with the metaphosphate to form insoluble and amorphous aluminum phosphates. The depletion of the soluble aluminum species caused further dissolution and precipitation. The precipitated aluminum phosphates have gellike structures that bond the alumina particles together and cause the viscosity of the suspensions to increase drastically. This phenomenon is termed bridging flocculation.<sup>22</sup> The chemical reaction and the reaction products are independent of the chain length.

Alumina is not soluble at neutral pH, and the particles are not highly charged. The negatively charged polymetaphosphates will adsorb to the alumina particle surfaces through hydrogen bonding and produce a negative charge on the particles. This will cause the viscosity of the suspensions to decrease. However, pure electrostatic repulsion cannot explain why the long-chain surfactant (Glass H) is more effective than the short-chain surfactant (Sodaphos). In fact, Figure 8 shows that, as far as the  $\zeta$  potential is concerned, the Sodaphos is better and the  $\zeta$  potential is slightly higher in the suspension that contains Sodaphos. The fact that the chain length matters implies that a steric effect is associated with the large molecules. The  $^{31}\text{P}$  NMR results indicate that the phosphate is bound to the particle surface through the end groups, and most of the middle-chain regions do not participate in the bonding. This implies that the surfactant chains extend out into the solution and provide the additional steric repulsion forces. Therefore, the stabilization of alumina suspensions by polymetaphosphate surfactants can be best described by electrosteric interactions.<sup>7</sup>

A portion of aluminum oxide was transformed to hydroxyaluminate at high pH. Polymetaphosphate surfactant began to

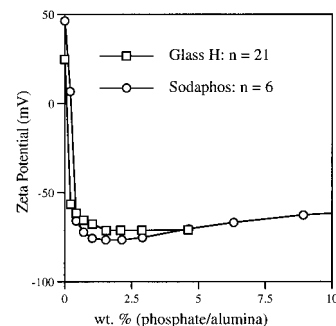


**Figure 8.**  $\zeta$  potential of alumina suspensions at neutral pH. Sodaphos is slightly more effective than Glass H.

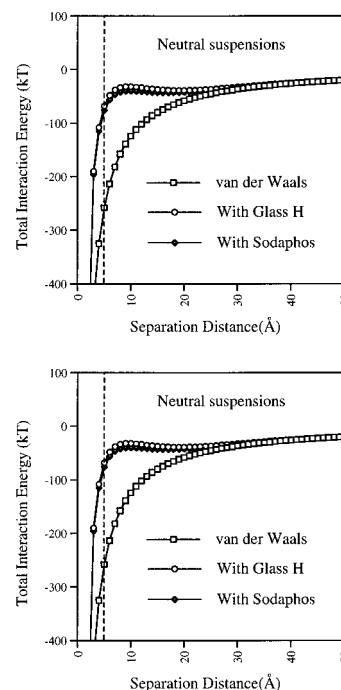


**Figure 9.** Interaction energies of alumina suspensions at neutral and high pH. (a) At neutral pH, the adsorption of the surfactants reduced the attraction energies. A steric barrier larger than 5 Å will be able to provide a shallow potential well and reduce the viscosities of the suspensions. (b) At high pH, the long-chain surfactant decomposed into short ones and no longer provided any steric effect. At the same time, the additional sodium ions introduced by the surfactants compressed the electrical double layer and increased the attraction energy.

degrade into shorter chains at the same time. The short chains did not provide sufficient steric repulsion to stabilize the suspension. On the other hand, adding polymetaphosphates increased the electrolyte concentration and reduced the effective electrical double-layer thickness. This in return modestly increased the viscosity of the suspensions. Because the viscosity increase is only related to the electrolyte concentration, Glass H and Sodaphos produced the same results.

An estimated magnitude of the interparticle energies also supported the conclusions reached so far. Without specific absorption, the total interaction energy contains two parts: a van der Waals attractive force and an electrostatic repulsive force.<sup>23</sup> In the neutral pH range, the particles were not highly charged and the van der Waals force dominated. Using an effective Hamaker constant of 16.3 kJ ( $6.7 \times 10^{-20}$  J),<sup>24</sup> the van der Waals attraction energy was calculated and plotted in Figure 9a. The suspension would be highly flocculated and had a high viscosity. When the metaphosphate surfactants were adsorbed onto the surface, the particles became negatively charged and had a  $\zeta$  potential of approximately 70 mV. Using

a constant potential approximation<sup>23</sup> and taking into account the screening effect from all nitrate and sodium ions (besides NaNO<sub>3</sub>, metaphosphate surfactant also contains sodium ions), the total interaction energies were calculated and overlaid onto Figure 9a. With the surfactant, the attractive energy decreased, and a wide plateau region was observed. However, under these conditions, no energetic barrier was observed, and the suspension is still prone to flocculation. The significantly reduced viscosity can only be explained if a steric repulsion term is introduced into the interaction potential, thereby allowing truncation of the curve before the particles fall into the primary minimum. The NMR data reported in this paper suggest that the long-chain surfactants indeed are partially anchored to the particle surface and produce a steric layer. Figure 9a also suggests that the thickness of this layer should be greater than 5 Å (below 5 Å, the attractive force increases rapidly), a requirement that can be met by Glass H, but not by Sodaphos. The Sodaphos has only six phosphorus segments and does not produce an effective steric layer on the particle surfaces.

The interaction energies were also calculated for basic suspensions, and the results are plotted in Figure 9b. The  $\zeta$  potential of the particles was measured to be about 50 mV. The suspension in basic solution was not stable without adding surfactant. Adding surfactant into the suspension increased the sodium ion concentration, which reduced the double-layer thickness around the particles. Hence, the electrostatic repulsion forces were reduced, and the total interaction potential became more attractive, which means increased viscosity for the suspensions. The NMR experiments also indicated that the metaphosphate surfactants dissociate into shorter molecules, thereby ruling out any steric effect. Therefore, the phosphate surfactant does not function as an effective dispersant at high pH.

**Acknowledgment.** Pacific Northwest National Laboratory is operated for the U.S. Department of Energy by Battelle under Contract DE-AC06-76RLO 1830. This work derives support through the Materials Science Division of Basic Energy Science,

U.S. Department of Energy. We thank Dr. Peter A. Smith at the Pacific Northwest National Laboratory for many useful discussions on phosphate chemistry.

## References and Notes

- (1) Faison, J.; Haber, R. A. *Ceram. Eng. Sci. Proc.* **1991**, 12, 106.
- (2) Nelson, R. D. *Dispersion Powders in Liquids*; Elsevier Sci B. V.: Amsterdam, The Netherlands, 1988; p 99.
- (3) For a review, see: Moreno, R. *Am. Ceram. Soc. Bull.* **1992**, 71, 1521, 1647.
- (4) Chou, K.-S.; Lee, L.-J. *J. Am. Ceram. Soc.* **1989**, 72, 1622.
- (5) Overbeek, J. Th. G. *J. Colloid Interface Sci.* **1977**, 58, 408.
- (6) Israelachvili, J. N. *Intermolecular and Surface Forces*; Academic Press: San Diego, CA, 1992; Chapters 11 and 12, and 14.
- (7) Cesarano, J.; Aksay, I. A. *J. Am. Ceram. Soc.* **1988**, 71, 370.
- (8) Exarhos, G. J.; Ferris, K. F.; Friedrich, D. M.; Samuels W. D. In *Atomic and Molecular Processing of Electronic and Ceramic Materials: Preparation, Properties, and Characterization. Proceedings of the Materials Research Society*; Materials Research Society, Pittsburgh, PA, 1988; pp 127–134.
- (9) Exarhos, G. J.; Ferris, K. F.; Friedrich, D. M.; Samuels W. D. *J. Am. Ceram. Soc.* **1988**, 71 (9), C406–7.
- (10) Martin, S. W. *Eur. J. Solid State Inorg. Chem.* **1991**, 28, 163.
- (11) Macdonald, J. C.; Mazurek, M. *J. Magn. Reson.* **1987**, 72, 48.
- (12) Hirohiko, W.; Hatano, M. *Polyhedron* **1982**, 1, 69.
- (13) Gard, D. R.; Burquin, J. C.; Gard, J. K. *Anal. Chem.* **1992**, 64, 557.
- (14) Quin, L. D.; Verkade, J. G., Eds. *Phosphorus-31 NMR Spectral Properties in Compound Characterization and Structural Analysis*; VCH: New York, 1994; p 364.
- (15) Pines, A.; Gibby, M. G.; Waugh, J. S. *J. Chem. Phys.* **1973**, 59, 569.
- (16) Voelkel, R. *Angew. Chem., Int. Ed. Engl.* **1988**, 27, 1468.
- (17) Lima, E.; Neto, J.; Fujiwara, F.; Galembeck, F. *J. Colloid Interface Sci.* **1995**, 176, 388.
- (18) Liu, J.; Wang, L. Q.; Bunker, B. C.; Graff, G. L.; Virden, J. W.; Jones, R. H. *Mater. Sci. Eng.* **1995**, A204, 169.
- (19) Brinker, C. J.; Scherer, G. W. *Sol–Gel Science*; Academic Press: San Diego, CA, 1990; p 60.
- (20) Baes, C. F., Jr.; Mesmer, R. E. *The Hydrolysis of Cations*; John Wiley & Sons: New York, 1976; Chapter 6.
- (21) Hanna, J. V.; Bradley, S. M. *J. Am. Chem. Soc.* **1994**, 116, 7771.
- (22) Kitchener, J. A. *Br. Polymer J.* **1972**, 4, 217.
- (23) Shaw, D. J. *Introduction to Colloid and Surface Chemistry*; Butterworths: Boston, MA, 1980; p 186.
- (24) Israelachvili, J. N. *Intermolecular and Surface Forces*; Academic Press: San Diego, CA, 1992; p 190.